Thesis for the degree of Master of Science

Simulation of the Maxwell-Dirac and Schrödinger-Poisson systems

by

Fredrik D. E. Johansson

Supervisor: **Nils Svanstedt**

Department of Mathematical Sciences
Chalmers University of Technology
Göteborg, Sweden, 2010

Abstract

We examine asymptotic and numerical aspects of the Dirac equation, with special attention to the Maxwell-Dirac (MD) system that arises when the time-dependent Dirac equation is coupled to Maxwell's equations for the electromagnetic field. In particular, we examine the nonrelativistic limit $c \to \infty$ where the full MD system can be approximated by the simpler Schrödinger-Poisson (SP) system by eliminating the singular dependence on c.

We give a detailed description of an efficient FFT-based pseudospectral method for numerical simulation of the MD and SP systems, and provide source code for an implementation in Matlab. Simulation results are shown for some test problems, comparing the MD system for large values of c with the asymptotic SP system and verifying the accuracy of the solver.

Acknowledgements

I want to express my deepest thanks to Nils Svanstedt for suggesting the subject of this thesis, providing valuable advice, and assisting with practical matters during the course of the work.

I am also in debt to the many outstanding teachers in courses on mathematics and physics for whom I have had the opportunity to study at Chalmers.

Finally, I would like to thank my friends and family for their support.

Contents

1 Background and theory

The Dirac equation, which is one of the staples of relativistic quantum mechanics, presents many interesting mathematical challenges. In this thesis, we will look at the so-called Maxwell-Dirac equations, with particular attention to the nonrelativistic limit where the speed of light c formally tends to infinity.

It is generally impossible to solve the Dirac equation exactly, so it must be studied using asymptotic methods or through numerical simulations. A prerequisite for performing numerical simulations of the nonrelativistic limit is to find an algorithm that is efficient and accurate in the asymptotic regime, a problem solved recently by Huang *et al.* in [3]. Before describing their algorithm in detail, we shall introduce the Dirac equation and provide some theoretical analysis of its asymptotics.

The Dirac equation constitutes a vast topic, most of which is outside the scope of this text. A more comprehensive general account of the Dirac equation can be found in the monograph by Thaller [9]; it is also covered in many advanced physics textbooks (see e.g. [8]). For our purposes, it will be sufficient to view the Dirac equation as an extension of the Schrödinger equation without studying issues of its physical interpretation in much more depth.

1.1 Introduction to the Dirac equation

Paul Dirac's discovery of the Dirac equation for the electron[1] in 1928 represented one of the first fruitful attempts to combine quantum mechanics with special relativity. Perhaps most significantly, Dirac's theory predicted the existence of antiparticles – positrons – which were detected experimentally four years later.

The problem that leads to the Dirac equation is to find a relativistically correct quantum mechanical equation for the electron. Quantum mechanics assumes that the state of a particle (or some more general system) is described by a complex-valued wavefunction $\psi(t, x)$, and that classical quantities must be supplanted by operators such as the energy operator

$$E = i\hbar\frac{\partial}{\partial t}$$

and the momentum operator

$$p = -i\hbar\nabla.$$

The fundamental equation of quantum mechanics, postulated to govern the behavior of any physical system, is the Schrödinger equation

$$E\psi = H\psi \tag{1}$$

[1]The Dirac equation has other applications, but for simplicity, we assume for the remainder of this text that it describes electrons.

where H is the Hamiltonian operator corresponding to the system. The Hamiltonian essentially describes the total energy of the system as the sum of kinetic and potential energy, and for a single (massive, spinless, nonrelativistic) particle takes the form

$$H = -\frac{p^2}{2m} + V. \tag{2}$$

Here $\hbar$ is the normalized Planck constant, m is the mass of the particle, and V is potential energy due e.g. to an external electromagnetic or gravitational field. Note that in (1) and (2), the symbols p and E denote the previously-defined operators. The measurable quantities "momentum" and "energy" actually correspond to eigenvalues of these operators, and phenomena such as quantization and the Heisenberg uncertainty principle are consequences of this operator formalism.

Returning to the non-quantum world where E and p are just numbers, the relativistic relation between energy and momentum reads $E^2 = c^2p^2 + m^2c^4$. Directly inserting the quantum operator versions of E and p into this equation gives the Klein-Gordon equation

$$\frac{1}{c^2}\frac{\partial^2}{\partial t^2}\psi - \nabla^2\psi + \frac{m^2c^2}{\hbar^2}\psi = 0, \tag{3}$$

which is useful in its own right but turns out not to satisfactorily solve the problem which Dirac sought to address. One of the issues is that the electron is known (from nonrelativistic quantum mechanics) to have *spin*. The Klein-Gordon equation does not contain any information about spin, so it cannot provide a complete description of the electron. It is also not first-order with respect to the time derivative, which is required for the mathematics of quantum mechanics (the function ψ in the Klein-Gordon equation cannot directly be interpreted as a wavefunction).

Dirac's approach to obtain a first-order, spin-aware version of the Schrödinger equation whose solution also satisfies the Klein-Gordon equation consisted of replacing the scalar wavefunction with a vector wavefunction. Then H should be a matrix operator. For algebraic reasons, it turns out that the wavefunction must be four-dimensional, i.e.

$$\psi = \begin{pmatrix} \psi_1 \\ \psi_2 \\ \psi_3 \\ \psi_4 \end{pmatrix} \in \mathbb{C}^4.$$

The four-dimensional complex-valued wave function is called a *Dirac spinor*. The Dirac Hamiltonian can be written in terms of 4-by-4 matrices. Explicitly, the *free Dirac operator* or *free Dirac Hamiltonian* is given by

$$H_0 \equiv D_0 \equiv c\alpha \cdot p + \beta mc^2 = -i\hbar c\, \alpha \cdot \nabla + \beta mc^2 \tag{4}$$

where $\alpha = (\alpha_1, \alpha_2, \alpha_3)$ and β, α_k are 4×4 matrices given by

$$\beta = \begin{pmatrix} \mathbb{I}_2 & 0 \\ 0 & -\mathbb{I}_2 \end{pmatrix} = \begin{pmatrix} 1 & 0 & 0 & 0 \\ 0 & 1 & 0 & 0 \\ 0 & 0 & -1 & 0 \\ 0 & 0 & 0 & -1 \end{pmatrix} \tag{5}$$

$$\alpha_k = \begin{pmatrix} 0 & \sigma_k \\ \sigma_k & 0 \end{pmatrix}; \quad \sigma_1 = \begin{pmatrix} 0 & 1 \\ 1 & 0 \end{pmatrix} \quad \sigma_2 = \begin{pmatrix} 0 & -i \\ i & 0 \end{pmatrix} \quad \sigma_3 = \begin{pmatrix} 1 & 0 \\ 0 & -1 \end{pmatrix}. \tag{6}$$

The σ_k matrices are also known as the Pauli matrices and occur in the nonrelativistic quantum-mechanical description of particles with spin. The need for a four-dimensional system is a consequence of the spin dependence in three-dimensional space: when $m = 0$, or when the particle is isolated to one or two spatial dimensions, the Dirac operator can be reduced to two dimensions and represented using Pauli matrices.

The wavefunction in the Schrödinger equation, or rather the wavefunction's squared magnitude, is usually interpreted as describing the location of a particle in space as a probability distribution. The *probability density* for the Dirac wavefunction (understood to represent an electron) is the pointwise quantity

$$|\psi(x)|^2 = \sum_{k=1}^{4} |\psi_k(x)|^2 \tag{7}$$

and the total probability to find the particle in some region $S \subseteq \mathbb{R}^3$ is

$$P(S) = \|\psi\|^2_{L^2(S)} = \int_S |\psi(x)|^2 dx \tag{8}$$

assuming that the wavefunction is normalized so that $P(\mathbb{R}^3) = 1$. With this interpretation, the Schrödinger equation (1) with the Dirac Hamiltonian defines how the Dirac particle evolves, i.e. how the distribution of probability density moves or spreads in space as time progresses.

1.2 Spectrum of the Dirac operator

Besides being a time-dependent equation, (1) can be understood an eigenvalue equation where the symbol E denotes the possible scalar energy eigenvalues that may be assumed by the wavefunction. An interesting property of the Dirac equation distinguishes it from the ordinary Schrödinger equation: it can be shown that the spectrum of the free Dirac operator, $\Gamma(H_0)$, is absolutely continuous and is the union of the intervals $(-\infty, -mc^2]$ and $[mc^2, \infty)$. The apparent paradox that a Dirac electron may have *negative energy* can be resolved by introducing antiparticles.

When $p \to 0$, the Dirac equation reduces to an "upper" and a "lower" part with respective energies $\pm mc^2$ (the relativistic rest energy of a particle with mass m). The upper part of the wavefunction

$$\psi_+ = \begin{pmatrix} \psi_1 \\ \psi_2 \\ 0 \\ 0 \end{pmatrix}$$

is usually interpreted as representing an electron, while the lower part

$$\psi_- = \begin{pmatrix} 0 \\ 0 \\ \psi_3 \\ \psi_4 \end{pmatrix}$$

is interpreted as representing a positron. The fact that the lower energy is negative accounts for the interpretation of the positron as an antiparticle. In general, however, all components of ψ are nonzero and the particle described by the Dirac equation must be understood as a complex superposition of an "electronic" and a "positronic" part. The 2-spinors ψ_+ and ψ_- are known as the Pauli spinors.

It is commonly accepted that the free Dirac equation describes a relativistic electron (or rather an oscillating electron-positron field) in free space. Adding a potential V to the free Dirac operator yields the Dirac equation in more general form,

$$E\psi = (H_0 + V)\psi. \tag{9}$$

The potential V can be a scalar $V = \varphi \mathbb{I}_4$ or more generally a 4×4 matrix (to model magnetic effects). For example, the electrostatic Coulomb potential V_C with

$$\varphi = \frac{C}{|x|}$$

is often used in the description of electronic orbits in point-nucleus atoms.

With a Coulomb potential V_C as above, eigenvalues appear in the gap, i.e. $\Gamma(H_0 + V_C) = \Gamma(H_0) \cup \{\lambda_k\}_{k=1}^{\infty}$. These eigenvalues can accumulate either at $-mc^2$ or at mc^2, and correspond to bound states of electrons or positrons. If we instead add a periodic potential V_{per}, $\Gamma(H_0 + V_{\text{per}})$ is purely absolutely continuous and consists of a countable set of disjoint intervals separated by gaps.

Much is unknown about the spectrum of the Dirac Hamiltonian with a more general potential, such as a sum of a Coulomb potential and a magnetic potential. Even proving the existence of the eigenvalues in a Coulomb potential is a delicate matter since the Dirac operator is unbounded and therefore no minimization principle exists (one way to overcome this deficiency is to work with the Pauli spinors). Questions about the existence and distribution of eigenvalues of Dirac operators, as well as numerical methods for finding eigenvalues, are subject of ongoing research (see e.g. [5]).

1.3 Time evolution and the Maxwell-Dirac equations

The Schrödinger equation can be interpreted both as an eigenvalue equation for the possible energy values of the Hamiltonian, and as a time-evolution differential equation for the wavefunction. In the remainder of this text, we will mainly be concerned with the latter point of view. In more detail, the Schrödinger equation states that a physical system described by a wavefunction $\psi = \psi(t) = \psi(t, x)$ and Hamiltonian operator H evolves in time as

$$i\hbar \frac{\partial}{\partial t}\psi(t) = H\psi(t). \tag{10}$$

Given an initial configuration $\psi(0, x) = \psi_0$, the solution can be represented exactly as

$$\psi(t) = e^{-iHt/\hbar}\psi_0 \tag{11}$$

where e^A denotes the exponential function of the operator A, given formally by the power series

$$e^A = \sum_{k=0}^{\infty} \frac{A^k}{k!} \qquad \text{i.e.} \qquad e^A\psi = \sum_{k=0}^{\infty} \frac{A^k}{k!}\psi. \tag{12}$$

In order for this expression to be meaningful, some restrictions must be imposed on A to guarantee convergence and that the limit operator resides in some suitable space. If A is an element of a (unital) Banach algebra $\mathcal{B}$ such as the space of $n \times n$ matrices over $\mathbb{C}$, then e^A is also an element of $\mathcal{B}$.

In quantum mechanics, it is always assumed that H is Hermitian (or self-adjoint). Under this assumption, a theorem proved by Stone [7] states that the family of operators $U(t) = e^{-iHt/\hbar}$ are unitary, satisfy $U(t_1 + t_2) = U(t_1)U(t_2)$, and are strongly continuous with respect to the real parameter t. The continuity property implies that (11) gives the desired unique solution of (10). The unitarity property is fundamental to the physics because it implies that the norm $\|\psi\|$ of the wavefunction, i.e. the total probability of finding the system in some configuration in space, is conserved in time.

Although (11) gives an elegant expression for the solution of the time-evolution problem, evaluating the operator exponential is difficult. Direct application of the series (12) is often impractical for qualitative analysis or computation when A is a differential or matrix operator. When studying the Dirac equation in more detail, we will use the Fourier transform and diagonalization (see appendix A) to overcome this difficulty.

The time-dependent version of the Dirac equation with a potential reads

$$i\hbar \frac{\partial}{\partial t}\psi = (H_0 + V)\psi. \tag{13}$$

The free Dirac Hamiltonian H_0 is self-adjoint (technically, essentially self-adjoint), so the free Dirac equation has a well-defined solution per Stone's theorem. The Dirac operator remains self-adjoint with the addition of a potential, subject to some regularity conditions on the

potential (see theorem 4.2 in [9]). For example, the Coulomb-Dirac Hamiltonian $H_0 + V_C$ is self-adjoint as long as the constant C is not too large.

In (13), V describes the electron's interaction with an *external* electromagnetic field. A more accurate description of the electron should account for its self-interaction due to the electromagnetic field it generates. This can be accomplished by combining the Dirac equation with Maxwell's equations, giving the coupled *Maxwell-Dirac (MD) system* (in Lorentz gauge)

$$i\hbar\frac{\partial}{\partial t}\psi = \left(-i\hbar c\alpha\cdot\nabla + mc^2\beta - q\alpha\cdot(\mathbf{A}+\mathbf{A}_{\text{ex}}) + (V+V_{\text{ex}})\right)\psi \tag{14}$$

$$\left(\frac{1}{c^2}\frac{\partial^2}{\partial t^2} - \Delta\right)V = \frac{1}{4\pi\epsilon_0}\rho$$

$$\left(\frac{1}{c^2}\frac{\partial^2}{\partial t^2} - \Delta\right)\mathbf{A} = \frac{1}{4\pi\epsilon_0 c}\mathbf{J}$$

The first equation is the Dirac equation with the interaction of both an electric potential (V) and a *magnetic vector potential* ($\mathbf{A}$) included. Here V denotes the self-consistent, i.e. self-generated field while V_{ex} denotes an externally applied field, and similarly with the the magnetic potential. Here $\mathbf{A} = (A_1, A_2, A_3)$ and $\mathbf{J} = (J_1, J_2, J_3)$ consist of three scalar fields.

The *densities* $\rho = q|\psi|^2$ and $J_k = qc\langle\psi, \alpha_k\psi\rangle_{\mathbb{C}^4} = qc\bar{\psi}\cdot\alpha_k\psi$ describe the flow of probability density and current respectively. Above, ϵ_0 denotes the permittivity of vacuum and q denotes the particle charge.

Unlike the free Dirac equation or the Dirac equation with a (sufficiently well-behaved) external potential, where Stone's theorem applies, only partial results are known concerning well-posedness, i.e. existence and uniqueness of solutions, of the Maxwell-Dirac equations.

1.4 The nonrelativistic limit

Two importantant asymptotic cases of the Dirac equation are the *semiclassical limit* $\hbar \to 0$ and the *nonrelativistic limit* $c \to \infty$. Roughly speaking, the semiclassical limit should recover the description of a relativistic particle for which quantum effects are negligible, and vice versa. Both limits are *singular*, which is to say that the equations become meaningless when $\hbar = 0$ or $c = \infty$. Any asymptotic analysis must therefore begin by describing the singular dependence of the problem on the limit parameter.

In fact, the singular asymptotics of the Maxwell-Dirac equations are well-studied and it is known that the MD system can be described in terms of simpler systems in the aforementioned limits. As $c \to \infty$, MD reduces to the *Schrödinger-Poisson* system, and the $\hbar \to 0$ limit gives the relativistic *Vlasov-Maxwell* system. The combined limit leads to the *Vlasov-Poisson* system. Details can be found in [4]. The semiclassical limit has also been investigated using WKB techniques, for which see [6]. From here on, our concern will be the nonrelativistic limit.

For mathematical analysis, it is convenient to eliminate the physical constants occurring in the Maxwell-Dirac system by introducing dimensionless parameters. As in [3], we may use

the two-parameter dimensionless version

$$i\epsilon\frac{\partial}{\partial t}\psi = \left(-\frac{i\epsilon}{\delta}\alpha\cdot\nabla + \frac{1}{\delta^2}\beta - \alpha\cdot(\mathbf{A}+\mathbf{A}_{\text{ex}}) + (V+V_{\text{ex}})\right)\psi \tag{15}$$

$$\left(\delta^2\frac{\partial^2}{\partial t^2} - \Delta\right)V = \epsilon|\psi|^2$$

$$\left(\delta^2\frac{\partial^2}{\partial t^2} - \Delta\right)A_k = \epsilon\langle\psi, \alpha_k\psi\rangle$$

where $\epsilon \to 0$ corresponds to the semiclassical limit and $\delta \to 0$ corresponds to the nonrelativistic limit. In other words, $\epsilon = C_1\hbar$ and $\delta = C_2 c^{-1}$, where the constants C_1 and C_2 depend on the units or reference length and time scales chosen.

A leading-order analysis of the nonrelativistic limit is straightforward. Starting from (15) with $\epsilon = 1$, and letting $\delta \to 0$, the term $\delta^{-2}\beta\psi$ dominates the right-hand side in the first line. Since β is diagonal, the equation

$$i\frac{\partial\psi}{\partial t} = \frac{1}{\delta^2}\beta\psi$$

has solution

$$\psi_{1,2}(t) = e^{-it/\delta^2}\psi_{1,2}(0)$$

$$\psi_{3,4}(t) = e^{+it/\delta^2}\psi_{3,4}(0).$$

This describes a wavefunction with rapid phase oscillation but whose probability density remains static and whose components $(\psi_1, \psi_2, \psi_3, \psi_4)$ do not interact with each other. As it turns out, this heuristic argument correctly identifies the most rapid variation of the solution depending on δ. When accounting for the remaining parts of the MD system, instead of $\psi_{1,2,3,4}(0)$ the right-hand side should contain a more slowly-varying time-dependent function that approximately solves the MD system with the $\delta^{-2}\beta\psi$-term subtracted.

For a more precise analysis, we rewrite the first equation of (15), again with $\epsilon = 1$, as

$$i\frac{\partial}{\partial t}\psi = (H_T + H_V)\,\psi \tag{16}$$

where $H_T \equiv H_T(\delta)$ is the scaled free Dirac operator, while H_V is the potential operator that does not depend on δ. We also take the Fourier transform of H_T, i.e.

$$H_T = \left(\frac{1}{\delta}\right)\alpha\cdot\xi + \frac{1}{\delta^2}\beta \tag{17}$$

where ξ is a Fourier space coordinate (see appendix A.1), and

$$H_V = (V + V_{\text{ex}}) - \alpha \cdot (\mathbf{A} + \mathbf{A}_{\text{ex}}). \tag{18}$$

Now H_T is an ordinary 4×4 matrix, and can be diagonalized (see appendix A.2). Solving the eigenvalue equation $|H_T - \lambda \mathbb{I}_4| = 0$ gives the eigenvalues $(\lambda, \lambda, -\lambda, -\lambda)$ where

$$\lambda = \frac{1}{\delta^2}\sqrt{1 + \delta^2 |\xi|^2}. \tag{19}$$

Therefore, up to multiplication by two unitary operators P and P^{-1} which transform H_T to diagonal form, H_T is equivalent to the diagonal operator

$$D = \beta\lambda \tag{20}$$

and the series expansion $\sqrt{1+x} = 1 + \frac{1}{2}x + \ldots$ gives

$$D = \beta\left(\frac{1}{\delta^2} + \frac{|\xi|^2}{2}\right) + O(\delta^2) \tag{21}$$

where the nonsingular term is the "ordinary Schrödinger equation Hamiltonian"

$$\mp\frac{\Delta}{2}$$

with negative and positive sign taken for the upper two and lower two components of the wavefunction respectively. We may next introduce the two respective *subspace projection operators*

$$\Pi_{e/p} = \frac{1}{2}\left(\mathbb{I}_4 \pm \frac{\delta\alpha \cdot \xi + \beta}{\sqrt{1 + \delta^2|\xi|^2}}\right).$$

These operators project the wavefunction onto the respective subspace of positive and negative energy, and inspection immediately shows that when $\delta \to 0$,

$$\Pi_e \to \begin{pmatrix} \mathbb{I}_2 & 0 \\ 0 & 0 \end{pmatrix}$$

and

$$\Pi_p \to \begin{pmatrix} 0 & 0 \\ 0 & \mathbb{I}_2 \end{pmatrix}$$

so the subspaces asymptotically correspond to the component subspaces $(\psi_1, \psi_2, 0, 0)$ and $(0, 0, \psi_3, \psi_4)$.

We now combine the Dirac equation with the Maxwell equations. Formally letting $\delta \to 0$ in the first of Maxwell's equations in (15) gives Poisson's equation for V, while the magnetic

field turns out to behave as $O(\delta)$ and therefore this field can be dropped entirely in the limit (this is due to a rather complicated cancellation effect). In summary, we obtain in the *Schrödinger-Poisson system*

$$i\frac{\partial}{\partial t}\phi_e = -\frac{\Delta}{2}\phi_e + (V + V_{ex})\phi_e, \tag{22}$$

$$i\frac{\partial}{\partial t}\phi_p = +\frac{\Delta}{2}\phi_p + (V + V_{ex})\phi_p,$$

$$-\Delta V = |\phi_e|^2 + |\phi_p|^2.$$

Here the "electronic" and "positronic" components relate to those of the Maxwell-Dirac wavefunction as $\psi_{e,p} \to \phi_{e,p}, \delta \to 0$ where

$$\psi_e = e^{it/\delta^2}\Pi_e\psi$$

$$\psi_p = e^{-it/\delta^2}\Pi_p\psi$$

i.e. with the singular dependence on δ factored out. Up to the phase, we therefore also have $\phi_e \to (\psi_1, \psi_2)$ and $\phi_p \to (\psi_3, \psi_4)$.

Although the derivation above is heuristic, the convergence of the Maxwell-Dirac system to the Schrödinger-Poisson system can be formulated and proven rigorously. The interested reader may consult [2].

2 Numerical algorithms

The Maxwell-Dirac equations constitute a coupled system of hyperbolic partial differential equations, presenting considerable difficulties for numerical algorithms and simulations. We will here apply a version of the *pseudospectral method*, which is attractive for a large class of PDEs due to providing high-order spatial accuracy and being relatively simple to formulate and implement, even in three spatial dimensions.

2.1 Spectral methods

Suppose we are interested in solving a differential equation on some domain S. The idea of a *spectral method* is to represent any occurring function f (the solution, initial data, etc.) as the sum of a Fourier series

$$f(x) = \sum_{k=0}^{\infty} c_k \phi_k(x) \approx f_N(x) = \sum_{k=0}^{N-1} c_k \phi_k(x) \tag{23}$$

where

$$c_k = \frac{1}{|S|} \int_S f(x) \overline{\phi_k(x)} dx \tag{24}$$

and where ϕ_k denote chosen basis functions. Besides the ordinary trigonometric or exponential Fourier basis functions, any suitable orthogonal set of simple basis functions for $L^2(S)$ can be used (e.g. orthogonal polynomials), giving a *generalized Fourier series*. Spectral methods are also related to *finite element methods* which use "nearly-orthogonal" piecewise basis functions.[2]

Using the representation (23)-(24) , the differential equation of interest can often be reduced to a solvable algebraic equation involving the Fourier coefficients c_k. Moreover, if f has suitable properties, $\|f - f_N\|$ decreases very rapidly as $N \to \infty$. In the case of ordinary Fourier series, if f is periodic and has n-th derivatives, then $|c_k|$ decreases at least as rapidly as k^{-n} when $k \to \infty$. If f is periodic and infinitely differentiable, the convergence order of the method is thus "better than n-th order" for any finite n. This property makes spectral methods highly accurate for certain classes of problems.

Any function, not necessarily periodic, can be approximated by a Fourier series, but the use of the Fourier basis naturally imposes periodic boundary conditions on the solutions of differential equations. To simulate a problem without periodicity, it is conventional to choose an enlargened computational domain and initial data that decreases rapidly towards the boundaries, for example Gaussian data.

We now assume that S is a finite symmetric interval, $S = [-L/2, L/2]$ for which the ordinary Fourier basis may be used. It is convenient to assume that N is even and re-index (23) as

[2]Spectral methods are sometimes considered a subset of finite element methods and called spectral finite element methods.

$$f(x) = \sum_{k=-\infty}^{\infty} c_k \phi_k(x) \approx f_N(x) = \sum_{k=-N/2+1}^{N/2} c_k \phi_k(x). \tag{25}$$

where the basis functions may be written

$$\phi_k(x) = e^{2\pi i k x/L}.$$

The *pseudospectral* method arises if we approximate (24) by a step sum over the uniformly spaced grid $(x_0, x_1, \ldots, x_{N-1})$,

$$x_k = -\frac{L}{2} + \frac{kL}{N}.$$

It can be shown that this choice of step sum preserves the accuracy order of the method, i.e. it is as good as using exact integration.[3] Then, up to a normalization constant, the vector $(c_0, c_1, \ldots, c_{N-1})$ is simply the *discrete Fourier transform* (DFT) of the vector of function values $(f(x_0), f(x_1), \ldots, f(x_{N-1}))$,

$$c_k = \sum_{n=0}^{N-1} f(x_n) e^{-\frac{2\pi i}{N} kn} \qquad k = 0, \ldots, N-1. \tag{26}$$

Likewise, the *inverse discrete Fourier transform* (IDFT) gives

$$f(x_n) = \frac{1}{N} \sum_{k=0}^{N-1} c_k e^{\frac{2\pi i}{N} kn} \qquad n = 0, \ldots, N-1. \tag{27}$$

The DFT and its inverse ostensibly involve about $O(N^2)$ operations. The key to efficiency of the pseudospectral method is that both can be computed more efficiently using the fast Fourier transform (FFT), in $O(N \log N)$ operations.[4] Optimized FFT routines, especially for N that is a power of two or has only small prime factors, are widely available in scientific software.

The possibility of using the standard forms (26) and (27) relies on a subtle wrap-around effect of the DFT. Extended to arbitrary values of k, the sequence $(f(x_k))$ is clearly periodic with period N, i.e. $f(x_{k+N}) = f(x_k)$, since f is assumed to extend periodically outside S. This periodicity also holds for the c_k coefficients, i.e. $c_k = c_{k+N}$ and in particular $c_{-N/2} = c_{N/2}$, as can easily be verified algebraically from the DFT formulas. The impossibility of separating out the higher frequency modes when using a finite number N of samples is a consequence of the sampling theorem. Therefore, when performing computations, the Fourier coefficients may be stored in an array with indices

[3] This follows from the Euler-Maclaurin summation formula.

[4] Strictly speaking, FFT denotes a family of related algorithms with $O(N \log N)$ complexity, rather than a specific algorithm.

$$[0, 1, \ldots, N-1] \quad \text{or} \quad [1, 2, \ldots, N]$$

while one must remember that the corresponding indices in (25) are

$$\left[0, 1, \ldots, \frac{N}{2} - 1, \frac{N}{2}, \ -\frac{N}{2} + 1, \ldots, -2, -1\right]. \tag{28}$$

The normalization convention for the DFT does not matter as long as the scaling is undone consistently by the inverse DFT, since we will only perform linear operations on transformed quantities.

The discussion of Fourier series on intervals is easily extended to three (or any finite number of) dimensions. On a box

$$\left[-\frac{L_1}{2}, \frac{L_1}{2}\right] \times \left[-\frac{L_2}{2}, \frac{L_2}{2}\right] \times \left[-\frac{L_3}{2}, \frac{L_3}{2}\right],$$

we may use basis functions

$$\phi_{k_1,k_2,k_3}(x_1, x_2, x_3) = \exp\left(2\pi i \left(\frac{k_1 x_1}{L_1} + \frac{k_2 x_2}{L_2} + \frac{k_3 x_3}{L_3}\right)\right) \tag{29}$$

and the corresponding multidimensional DFT

$$c_{k_1,k_2,k_3} = \sum_{n_1=0}^{N_1-1} \sum_{n_2=0}^{N_2-1} \sum_{n_3=0}^{N_3-1} f_{n_1,n_2,n_3} \exp\left(-2\pi i \left(\frac{k_1 n_1}{N_1} + \frac{k_2 n_2}{N_2} + \frac{k_3 n_3}{N_3}\right)\right) \tag{30}$$

with inverse

$$f_{n_1,n_2,n_3} = \frac{1}{N_1 N_2 N_3} \sum_{k_1=0}^{N_1-1} \sum_{k_2=0}^{N_2-1} \sum_{k_3=0}^{N_3-1} c_{k_1,k_2,k_3} \exp\left(2\pi i \left(\frac{n_1 k_1}{N_1} + \frac{n_2 k_2}{N_2} + \frac{n_3 k_3}{N_3}\right)\right). \tag{31}$$

Both (30) and (31) can be evaluated by nested one-dimensional FFTs, although specialized multidimensional FFT algorithms exist that take better advantage of the data order in memory. In Matlab, e.g., the `fftn` and `ifftn` functions may be used.

The DFT and IDFT are approximations of the continuous Fourier transform and its inverse. This follows by the fact that the coefficients in the Fourier series of a periodic function f essentially are the lattice point values of $\hat{f}$. Strictly speaking, the continuous Fourier transform of a periodic function diverges, so this correspondence should be understood in a limiting or distributional sense ($\hat{f}$ is a sum of Dirac delta functions with the Fourier series coefficients as multipliers).

In terms of the coefficient indices k, the *discrete Fourier space coordinates* are

$$\xi_k = \frac{2\pi k}{L}$$

or in three dimensions,

$$\xi_k = \xi_{k_1,k_2,k_3} = \left(\frac{2\pi k_1}{L_1}, \frac{2\pi k_2}{L_2}, \frac{2\pi k_3}{L_3}\right).$$

Since

$$\phi_k'(x) = \frac{2\pi i k}{L}\phi_k(x) = i\xi_k\phi_k$$

it is easy to see that the discrete Fourier transform allows us replace differential operators with multiplication operators involving ξ, equivalent to those for the continuous Fourier transform (see appendix A.1). From here on, we will freely use $\mathcal{F}(f)$ or $\hat{f}$ to refer to either the exact Fourier transform of a wavefunction or the numerical DFT approximation of its samples.

2.2 The pseudospectral method for Schrödinger-type equations

We now turn to the problem of solving the Schrödinger-type equation (10)

$$i\hbar\frac{\partial}{\partial t}\psi(t) = H\psi(t),$$

that is, evaluating $\psi(t) = e^{-iHt/\hbar}\psi_0$. Approximating the operator exponential explicitly by means of the series (12) is impractical except for special H due to the fact that the higher powers of operators are complicated. Accordingly, some simplification must be employed.

One approach is to truncate (12) after the n-th order term and take a succession of small time steps. If the step length is τ, then the local error is of order $O(\tau^{n+1})$. In particular, $n = 1$ simply yields the forward (or explicit) Euler finite difference method in time for (10).

A second approach rests on the possibility of decomposing the Hamiltonian into $H = T + V$ where T is a differential operator (describing the kinetic energy of the system) and V is a multiplication operator (describing the potential energy due to interaction with external fields). Assuming that T can be diagonalized in Fourier space and V can be diagonalized in ordinary space, their exponentials can be computed separately.

This suggests using

$$e^{-i(T+V)t/\hbar} \approx e^{-iTt/\hbar}e^{-iVt/\hbar} \tag{32}$$

which is approximate since $e^{A+B} = e^Ae^B$ does not generally hold unless A and B commute. However, if t is small enough this is a good approximation. The time discretization error can be estimated using the Baker-Campbell-Hausdorff formula, and turns out to be of order $O(t^2)$.

Choosing a small time step τ and applying this to (11) gives

$$\psi(t+\tau) = e^{-i(T+V)\tau/\hbar}\psi_0 \approx \mathcal{F}^{-1}\left(e^{-iT\tau/\hbar}\mathcal{F}\left(e^{-iV\tau/\hbar}\psi(t)\right)\right). \tag{33}$$

Alternatively, a method with $O(\tau^3)$ error is obtained by choosing the symmetric decomposition

$$\psi(t+\tau) \approx e^{-iV\tau/(2\hbar)}\mathcal{F}^{-1}\left(e^{-iT\tau/\hbar}\mathcal{F}\left(e^{-iV\tau/(2\hbar)}\psi(t)\right)\right). \tag{34}$$

This is also known as the Strang-splitting method. Combined with a way to compute the Fourier transform, typically FFT, (33) or (34) defines a pseudospectral method for solving (10).

In the ordinary Schrödinger equation for a scalar wavefunction, V and T are immediately diagonal in the respective spaces. For the Dirac equation, we need to diagonalize 4×4 matrix operators.

2.3 Example: the 1D Schrödinger equation

As an illustration, we state the pseudospectral method for the ordinary Schrödinger equation with Hamiltonian

$$H = -\frac{\hbar^2}{2m}\frac{\partial^2}{\partial x^2} + V \equiv T + V$$

describing a particle with mass m in one dimension. We have

$$\mathcal{F}[T] = \frac{\hbar^2|\xi|^2}{2m}.$$

Let the domain be $[-L/2, L/2]$ with N sample points $[x_0, x_1, \ldots, x_{N-1}]$, and let

$$\xi = \frac{2\pi}{L}[0, 1, \ldots, N/2-1, N/2, -N/2+1, \ldots, -2, 1].$$

Given the sampled wavefunction $\psi_n = \psi(t_n)$, we obtain $\psi_{n+1} = \psi(t_{n+1})$ where $t_{n+1} = t_n + \tau$ using the following sequence of operations:

1. Compute $\hat{\psi}_n$ using FFT of ψ_n.
2. Compute the pointwise product $\hat{\phi} = e^{-i\tau\hbar\xi^2/(2m)}\hat{\psi}_n$.
3. Compute ϕ using inverse FFT of $\hat{\phi}$.
4. Compute the pointwise product $\psi_{n+1} = e^{-iV\tau/\hbar}\phi$.

The symmetric version is analogous, with one extra FFT and pointwise multiplication step.

2.4 Details for the Maxwell-Dirac system

We now state the time-splitting pseudospectral method introduced for the Maxwell-Dirac system in [3]. The following derivation is slightly more detailed and corrects a few minor typographical errors in the formulas of [3]. For reference, a related method with an alternative approach to the integration of Maxwell's equations is given in [1].

The algorithm for MD is similar to the previously-described method for the Schrödinger equation, with a two-step update of the wavefunction. The generated electromagnetic potential is updated in an intermediate step. We decompose the Maxwell-Dirac Hamiltonian in (15) as $H_T + H_V$ where

$$H_T = -\left(\frac{i\epsilon}{\delta}\right)\alpha \cdot \nabla + \frac{1}{\delta^2}\beta \tag{35}$$

and

$$H_V = (V + V_{\text{ex}}) - \alpha \cdot (\mathbf{A} + \mathbf{A}_{\text{ex}}). \tag{36}$$

Let t_n be the starting time and let $t_{n+1} = t_n + \tau$. We suppose that $\psi_n, V_n, V_n', \mathbf{A}_n, \mathbf{A}_n'$ (where primes denote time derivatives) are given for time t_n and V_{ex}, $\mathbf{A}_{\text{ex}}$ for time t_{n+1}. For clarity, let $\mathbf{\Psi}_n = \psi(t_n)$ denote the numerical approximation of the wavevector at time t_n and let $\mathbf{\Phi}_{n+1}$ denote the intermediate result from the splitting of the Hamiltonian. Then the following sequence of operations numerically solves the MD equations for time t_{n+1}:

- Compute $\hat{\mathbf{\Psi}}_n = \mathcal{F}[\mathbf{\Psi}_n]$.
- (Step 1): Solve $i\epsilon\psi' = H_T\psi$ in Fourier space, i.e. compute $\hat{\mathbf{\Phi}}_{n+1} = \exp(-iH_T\tau/\epsilon)\hat{\mathbf{\Psi}}_n$.
- (Step 2): Solve Maxwell's equations, i.e. compute $V_{n+1}, V_{n+1}', A_{n+1}, A_{n+1}'$ using the Crank-Nicolson time-stepping method in Fourier space.
- Compute $\mathbf{\Phi}_{n+1} = \mathcal{F}^{-1}[\hat{\mathbf{\Phi}}_{n+1}]$.
- (Step 3): Solve $i\epsilon\psi' = H_V\phi$ in real space, i.e. compute $\mathbf{\Psi}_{n+1} = \exp(-iH_V\tau/\epsilon)\mathbf{\Phi}_{n+1}$.

The details of steps 1, 2 and 3 are given in the following sections.

2.4.1 Computing the H_T and H_V exponentials

Defining $\mathbf{M}_1 = -iH_T\tau/\epsilon$, our goal is to find an exact representation for the 4×4 matrix $\exp(\mathbf{M}_1)$ by diagonalizing $\mathbf{M}_1$. Explicitly, moving to Fourier space where $\nabla = i\xi$,

$$\mathbf{M}_1 = \frac{\tau}{\delta}\begin{pmatrix} -a & 0 & -i\xi_3 & -i\xi_1 - \xi_2 \\ 0 & -a & -i\xi_1 + \xi_2 & i\xi_3 \\ -i\xi_3 & -i\xi_1 - \xi_2 & a & 0 \\ -i\xi_1 + \xi_2 & i\xi_3 & 0 & a \end{pmatrix}$$

where $a = i/(\delta\epsilon)$. By solving the characteristic equation $|\mathbf{M}_1 - \lambda\mathbb{I}_4|$, we find that $\mathbf{M}_1$ has four pure imaginary eigenvalues $(\lambda, \lambda, -\lambda, -\lambda)$ where

$$\lambda = \frac{i\tau}{\epsilon\delta^2}\sqrt{1 + \epsilon^2\delta^2|\xi|^2}$$

and therefore, letting $c = \cos(\lambda/i)$, $s = \sin(\lambda/i)$,

$$e^D = \begin{pmatrix} c+is & 0 & 0 & 0 \\ 0 & c+is & 0 & 0 \\ 0 & 0 & c-is & 0 \\ 0 & 0 & 0 & c-is \end{pmatrix}.$$

It is now straightforward, if tedious work, to compute expressions for P and P^{-1} by solving for each eigenvector, and then obtaining $e^{\mathbf{M}_1}$ by multiplying out Pe^DP^{-1}. Letting $\omega = \epsilon\delta\xi$ and $t = s(1 + |\omega|^2)^{-1/2}$, the result is

$$e^{\mathbf{M}_1} = \begin{pmatrix} c-it & 0 & -is\omega_3 & -s(\omega_2 + i\omega_1) \\ 0 & c-it & s(\omega_2 - i\omega_1) & is\omega_3 \\ -is\omega_3 & -s(\omega_2 + i\omega_1) & c+it & 0 \\ s(\omega_2 - i\omega_1) & is\omega_3 & 0 & c+it \end{pmatrix}. \tag{37}$$

To reliably arrive at this formula, a computer algebra system such as Mathematica (which uses diagonalization internally to evaluate symbolic matrix exponentials) may be used. Mathematica performs the algebra without eliminating common subexpressions, so the resulting formulas for the matrix entries are extremely long, but they can be obtained in a concise form using the following code:

```
a1 = {{0,0,0,1}, {0,0,1,0}, {0,1,0,0}, {1,0,0,0}}
a2 = {{0,0,0,-I}, {0,0,I,0}, {0,-I,0,0}, {I,0,0,0}}
a3 = {{0,0,1,0}, {0,0,0,-1}, {1,0,0,0}, {0,-1,0,0}}
B = {{1,0,0,0}, {0,1,0,0}, {0,0,-1,0}, {0,0,0,-1}}
DT = (-I e/d)(a1 I xi1 + a2 I xi2 + a3 I xi3) + (1/d^2)B
M1 = -I DT t / e
assumptions = And[t>0, d>0, e>0, xi1^2>0, xi2^2>0, xi3^2>0]
FullSimplify[Refine[MatrixExp[M1][[j,k]], assumptions]]
```

Likewise, we compute the exponential of $\mathbf{M}_2 = -iH_V\tau/\epsilon$. Temporarily writing V for $V + V_{\text{ex}}$ and A for $A + A_{\text{ex}}$,

$$\mathbf{M}_2 = \frac{\tau}{\epsilon}\begin{pmatrix} -iV & 0 & iA_3 & iA_1 + A_2 \\ 0 & -iV & iA_1 - A_2 & -iA_3 \\ iA_3 & iA_1 + A_2 & -iV & 0 \\ iA_1 - A_2 & -iA_3 & 0 & -iV \end{pmatrix} \tag{38}$$

and the eigenvalues are $(\lambda_1, \lambda_1, \lambda_2, \lambda_2)$ where

$$\lambda_1 = \frac{i\tau}{\epsilon}(-|\mathbf{A}| - V)$$

$$\lambda_2 = \frac{i\tau}{\epsilon}(|\mathbf{A}| - V)$$

and $|\mathbf{A}| = \sqrt{A_1^2 + A_2^2 + A_3^2}$.

With Mathematica, the elements of $\exp(\mathbf{M}_2)$ can be obtained in reasonably simple form using

```
HV = V - (a1 A1 + a2 A2 + a3 A3)
M2 = -I HV t / e
assumptions = And[A1^2>0, A2^2>0, A3^2>0, e>0, t>0]
Simplify[ExpToTrig[
  Expand[FullSimplify[
    ComplexExpand[
     Refine[Simplify[MatrixExp[M2]], assumptions][[j,k]]]]]]]
```

Let $u = |\mathbf{A}|\tau/\epsilon$, $v = \tau V/\epsilon$, and let $s_u = \sin u, c_u = \cos u, s_v = \sin v, c_v = \cos v$. Further, let $B_k = A_k/|\mathbf{A}| = A_k(A_1^2 + A_2^2 + A_3^2)^{-1/2}$ with the understanding that $B_k = 0$ when $|\mathbf{A}| = 0$. Next, let $a = c_v - is_v$ and $b = ic_v + s_v$. Then,

$$e^{\mathbf{M}_2} = \begin{pmatrix} c_u a & 0 & B_3 s_u b & (iB_1 + B_2)s_u a \\ 0 & c_u a & (B_1 + iB_2)s_u b & -iB_3 s_u a \\ B_3 s_u b & (iB_1 + B_2)s_u a & c_u a & 0 \\ (B_1 + iB_2)s_u b & iB_3 s_u a & 0 & c_u a \end{pmatrix}. \tag{39}$$

Note that formula for this matrix given in [3] (2.25-2.26) does not appear to be correct.

The code implementations of both $e^{\mathbf{M}_1}$ and $e^{\mathbf{M}_2}$ may be verified by comparing results for randomly chosen inputs with the output of e.g. Matlab's `expm` (which uses Padé approximants to compute matrix exponentials). Although `expm` can also be used directly in the algorithm, this is very slow compared to the use of exact formulas for large numbers of evaluation points.

2.4.2 Solving Maxwell's equations

If we Fourier transform the potentials and current densities, the Maxwell equations in the MD system simplify to a set of four simultaneous second-order ODEs in time (one ODE for each $f \in \{V, A_1, A_2, A_3\}$). Letting $\hat{f}$ denote the Fourier transform of f, the transformed equations read

$$\left(\delta^2 \frac{\partial^2}{\partial t^2} + |\xi|^2\right) \widehat{V} = \epsilon \widehat{|\psi|^2} \tag{40}$$

$$\left(\delta^2 \frac{\partial^2}{\partial t^2} + |\xi|^2\right) \widehat{A_k} = \epsilon \widehat{\langle \psi, \alpha_k \psi \rangle} \quad k = 1, 2, 3 \tag{41}$$

Since they are second-order, the values of both f and $f' = \partial_t f$ must be given as initial data at time t_n. We now reduce (40)-(41) to first-order ODEs by expressing them in terms of the vector variables $g = (\widehat{f}, \widehat{f'})$. For each equation (40), (41) with respective right-hand side $\hat{v}$, the reduced system reads

$$\mathbf{R}g' + \mathbf{S}g = \mathbf{v} \tag{42}$$

where

$$\mathbf{R} = \begin{pmatrix} 1 & 0 \\ 0 & \delta^2 \end{pmatrix} \qquad \mathbf{S} = \begin{pmatrix} 0 & -1 \\ 0 & |\xi|^2 \end{pmatrix} \qquad \mathbf{v} = \begin{pmatrix} 0 \\ \hat{v} \end{pmatrix}. \tag{43}$$

To solve an ODE in the standard form (42), a one-step finite difference method can be used. Suppose we know $g(t_n)$ and wish to approximate $g(t_{n+1})$. Letting $\tau = t_{n+1} - t_n$, $g_n = g(t_n)$, $\mathbf{v}_n = \mathbf{v}(t_n)$, using the finite difference approximation

$$g'(t) \approx \frac{g_{n+1} - g_n}{\tau} \quad t \in [t_n, t_{n+1}]$$

and elsewhere in (42) approximating $(g(t), \mathbf{v}(t))$ on $[t_n, t_{n+1}]$ as a weighted combination of $(g_n, \mathbf{v}_n)$ and $(g_{n+1}, \mathbf{v}_{n+1})$ gives the equation for the *generalized midpoint method*

$$\mathbf{R}\left(\frac{g_{n+1} - g_n}{\tau}\right) + \mathbf{S}(\theta g_{n+1} + (1-\theta)g_n) = \theta \mathbf{v}_{n+1} + (1-\theta)\mathbf{v}_n \tag{44}$$

where the weight $\theta \in [0, 1]$ may be chosen freely. Standard choices are $\theta = 0$ (the explicit or forward Euler method), $\theta = 1$ (the implicit or backward Euler method) and $\theta = 1/2$ (the midpoint or Crank-Nicolson method). The Crank-Nicolson method is suggested by [3] due to its stability properties for wave equations and demonstrated accuracy in numerical simulations of the similar Zakharov system.

Solving for g_{n+1} in (44) with $\theta = 1/2$ gives

$$g_{n+1} = \left(\mathbf{R} + \frac{\tau}{2}\mathbf{S}\right)^{-1} \left(\frac{\tau}{2}\left(\mathbf{v}_n + \mathbf{v}_{n+1}\right) + \left(\mathbf{R} - \frac{\tau}{2}\mathbf{S}\right) g_n\right) \tag{45}$$

which, evaluated explicitly for the MD system, becomes

$$\begin{pmatrix} \hat{V}_{n+1} \\ \hat{V}'_{n+1} \end{pmatrix} = \mathbf{C} \begin{pmatrix} \hat{V}_n \\ \hat{V}'_n \end{pmatrix} + \mathbf{D}\hat{\rho} \tag{46}$$

$$\begin{pmatrix} \widehat{(A_k)}_{n+1} \\ \widehat{(A'_k)}_{n+1} \end{pmatrix} = \mathbf{C} \begin{pmatrix} \widehat{(A_k)}_n \\ \widehat{(A'_k)}_n \end{pmatrix} + \mathbf{D}\hat{J}_k \quad k = 1, 2, 3 \tag{47}$$

with

$$\mathbf{C} = \frac{1}{r}\begin{pmatrix} 1 - \dfrac{\tau^2|\xi|^2}{4\delta^2} & \tau \\ -\dfrac{\tau|\xi|^2}{\delta^2} & 1 - \dfrac{\tau^2|\xi|^2}{4\delta^2} \end{pmatrix}, \qquad \mathbf{D} = \frac{\epsilon\tau}{4r\delta^2}\begin{pmatrix} \tau \\ 2 \end{pmatrix} \tag{48}$$

where

$$r = \left(1 + \frac{\tau^2|\xi|^2}{4\delta^2}\right) \tag{49}$$

and

$$\hat{\rho} = \mathcal{F}\left(|\mathbf{\Psi}_n|^2 + |\mathbf{\Phi}_{n+1}|^2\right) \tag{50}$$

$$\hat{J}_k = \mathcal{F}\left(\langle \mathbf{\Psi}_n, \alpha_k \mathbf{\Psi}_n\rangle + \langle \mathbf{\Phi}_{n+1}, \alpha_k \mathbf{\Phi}_{n+1}\rangle\right) \quad k = 1, 2, 3. \tag{51}$$

In summary, this step of the numerical algorithm consists of evaluating (50), (51), then (46) and (47), and finally obtaining V_{n+1}, V'_{n+1}, $(A_k)_{n+1}$ and $(A'_k)_{n+1}$ via inverse Fourier transform. For a slight efficiency improvement, the matrices $\mathbf{C}$ and $\mathbf{D}$ may be precomputed if τ is fixed. However, the eight total FFTs comprise the bulk of the work.

2.5 The Schrödinger-Poisson system

The Schrödinger-Poisson system can be solved using a pseudospectral method similar to that for the Maxwell-Dirac system, with a decomposition of the Hamiltonian and update of the potential V in an intermediate step. The main simplification is that, as with the ordinary Schrödinger equation, all operations (particularly exponentials) are scalar since the wavefunction components only interact via their influence on V. Since Poisson's equation does not involve any time derivatives, the step to update V also becomes simpler.

We solve the SP system for a time step τ by the following sequence of operations, given ϕ_e and ϕ_p as initial data, and given the external potential V_{ex}:

1. Update the wavefunction by the differential term of the Hamiltonian:

$$\chi_e = \mathcal{F}^{-1}\left[\exp\left(-\frac{1}{2}i|\xi|^2\tau\right)\mathcal{F}\left[\phi_e(t)\right]\right],$$

$$\chi_p = \mathcal{F}^{-1}\left[\exp\left(\frac{1}{2}i|\xi|^2\tau\right)\mathcal{F}\left[\phi_p(t)\right]\right].$$

2. Update the potential (solve Poisson's equation):

$$V = \mathcal{F}^{-1}\left[\frac{1*}{|\xi|^2}\mathcal{F}\left[|\chi_e|^2 + |\chi_p|^2\right]\right].$$

3. Update the wavefunction by the potential term of the Hamiltonian:

$$\phi_{e/p}(t+\tau) = \exp\left(-i\tau\left(V + V_{\text{ex}}\right)\right)\chi_{e/p}.$$

Above, $*$ signifies that an arbitrary value is chosen for zero mode $|\xi|^2 = 0$, e.g. zero.

2.6 Analysis of the algorithms

Due to the general properties of the pseudospectral method, the algorithms we have given for the Maxwell-Dirac and Schrödinger-Poisson systems can be expected to permit high-accuracy simulations. For asymptotic studies of the MD system, the pseudospectral method has some particularly useful features.

Firstly, since we solve the separate equations $i\epsilon\psi' = H_T\psi$ and $i\epsilon\psi' = H_V\psi$ exactly, the method exactly (up to floating-point roundoff) conserves the wavefunction norm. The same is also true for the Schrödinger-Poisson system.

Secondly, the pseudospectral method remains stable in the asymptotic regime $\delta \to 0$, again since we compute $\exp(-iH_T\tau/\epsilon)$ exactly. According with the asymptotic analysis, the nonsingular part of this matrix converges to the update matrix for the Schrödinger-Poisson system, with error which can shown to be $O(\delta)$.

The pseudospectral method for the Schrödinger-Poisson system has the main advantage over MD of being considerably simpler to implement, and it requires less computation per step since there are fewer FFTs to perform. Both systems have the same $O(N \log N)$ complexity per step, however.

3 Simulation results

We now present some results of numerical simulations of the Maxwell-Dirac and Schrödinger-Poisson equations. The simulations were performed using Matlab implementations of the algorithms described in the previous section. Source code is given in appendix C.

In all the following simulations, the domain is the unit cube $[-\frac{1}{2}, \frac{1}{2}]^3$ for simplicity. We use the same number N of grid points in each dimension, and denote the time step by τ. To minimize aliasing effects, we only choose periodic smooth initial data and external fields.

As a first "sanity test", the MD solver was tested on a specially chosen system with plane wave initial data as given in [1] and [3]. By choosing time-dependent external potentials that exactly cancel out the generated potentials, the wavefunction equation reduces to the free Dirac equation with plane wave solution, for which the pseudospectral method gives exact solution. Likewise, the Crank-Nicolson method gives exact solution for the Maxwell equations when the particle density is constant. The code was tested to give the exact solution to within floating-point roundoff error of about 10^{-13}.

3.1 Interaction of components

As a first investigation of the Maxwell-Dirac system in the nonrelativistic limit, we look at how the probability density moves between the upper (electronic) and lower (positronic) parts of the wavefunction. We choose a smooth well-like potential $V_{\text{ex}} = 50 \sin^4(\pi x) \sin^4(\pi y)$, $\mathbf{A}_{\text{ex}} = 0$, along with zero initial generated potentials

$$V = V' = \mathbf{A} = \mathbf{A}' = 0$$

and a smooth initial wavefunction

$$\psi = (f, 0, 0, 0)^T$$

where

$$f = \cos^2(\pi(x + 0.1)) \cos^2(\pi(y + 0.1)).$$

Here the initial probability density is concentrated entirely in the upper part of the wavefunction. The result of simulations with some different values of δ is shown in figure 1, demonstrating very clearly how the probability oscillates between the upper and lower parts.

With $\delta = 1$, the distribution quite rapidly stabilizes around a probability of $1/2$ for both the upper and lower parts. As δ decreases, the particle becomes increasingly confined to the upper subspace. The rate of the oscillation can also be seen to become more rapid and more chaotic. Different patterns and stabilization values can be obtained by choosing different initial data and potentials, but the general results are the same (c.f. figure 4 in [1]).

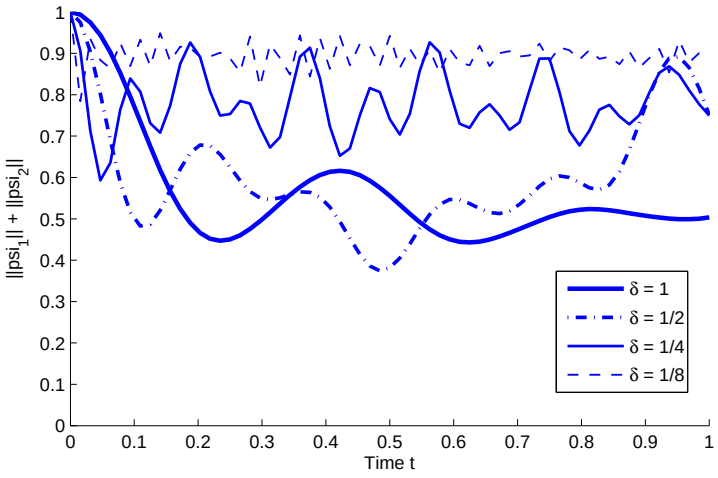

Figure 1: Interaction of the upper and lower components of the Dirac wavefunction. The graphs show the total probability for the upper part of the wavefunction, $y = \|\psi_1\| + \|\psi_2\|$, for different values of the nonrelativistic parameter $\delta \sim c^{-1}$. The corresponding probability for the lower part, not drawn, is the mirror quantity $1 - y$. Simulations were performed with $N = 24, \tau = 1/64$ and verified with $N = 32, \tau = 1/128$.

3.2 Comparison of MD and SP

We compare the MD and SP systems for small δ, verifying both that the algorithm for MD is accurate for extremely small parameter values and that the time evolution of MD is well approximated by the time evolution of the SP system. We choose initial wavefunctions

$$\psi_1 = \phi_e = \cos^4(\pi(x + 0.1)) \cos^4(\pi(y + 0.1))$$

$$\psi_3 = \phi_p = \cos^4(\pi(x - 0.1))^4 \cos^4(\pi(y - 0.1))$$

$$\psi_2 = \psi_4 = 0$$

Setting two components for zero in MD us lets us work with scalar-valued ϕ_e and ϕ_p in SP. We also choose zero initial potentials and set $V_{\text{ex}} = 100 \sin^4(\pi x) \sin^4(\pi y)$, $\mathbf{A}_{\text{ex}} = 0$.

Three snapshots at time $t = 0.25$, $t = 0.75$ and $t = 1.0$ with $\delta = 1/100$ are shown in figures 4, 5, and 6 in appendix B. Visual inspection shows that the probability amplitudes for the two systems distributed almost identically over the simulation timespan. Precise estimates of the difference between the systems as a function of time are plotted in figures 2 and 3 with $\delta = 1/100$ and $\delta = 1/1000$ respectively. Note the different scales on the y axis.

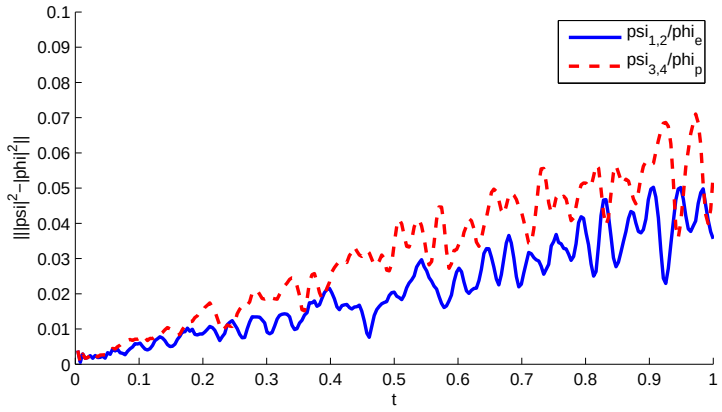

Figure 2: Norm of the difference in probability amplitudes between MD ($\delta = 1/100$) and SP with. The y axis shows $\||\psi_{1,2}|^2 - |\phi_e|^2\|$ and $\||\psi_{3,4}|^2 - |\phi_p|^2\|$.

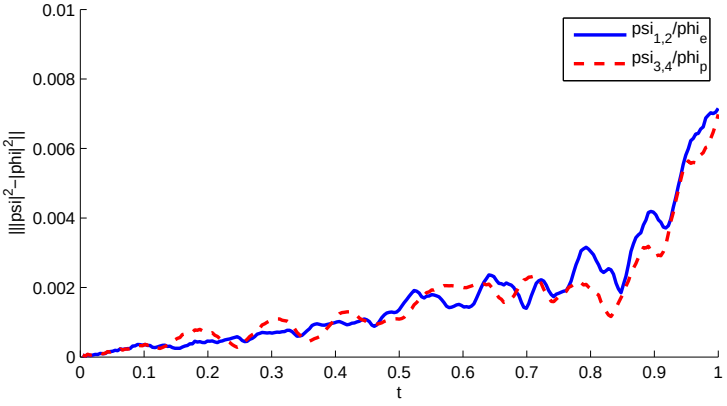

Figure 3: Norm of the difference in probability amplitudes between MD ($\delta = 1/1000$) and SP with. The y axis shows $\||\psi_{1,2}|^2 - |\phi_e|^2\|$ and $\||\psi_{3,4}|^2 - |\phi_p|^2\|$.

4 Discussion

We have seen that the Maxwell-Dirac equations, though a very hard system to study in full generality, can be analyzed effectively in the nonrelativistic limit $c \to \infty$ ($\delta \to 0$). Our numerical simulations confirm that the MD system with small values of δ is well-approximated by the simpler Schrödinger-Poisson system. The results suggest that, at least in some applications of the Dirac equation, it may be possible to work with the more well-behaved SP system instead of the MD system. Our simulations also confirm that the algorithm introduced by Huang *et al.* performs very well, at least for simple test problems, and likely also can be adapted to solve other, similar, singular asymptotic problems.

Much further work is possible. The numerical MD system has enormously many degrees of freedom: choice of initial data, choice of potentials, the semiclassical and nonrelativistic parameters, number of space dimensions, and space/time resolution. Much further work can be done studying variations in any of these. Many properties of the solution, such as the fine structure of the magnetic field, would also be interesting to study in more detail. It may also be interesting to compare the pseudospectral method with other algorithms, for instance finite difference and finite element methods.

A Mathematical tools

A.1 The Fourier transform

One of the most important tools in the mathematics of quantum mechanics, and not least in the study of the Dirac equation, is the Fourier transform. We let $\mathcal{F}(f)$ or $\hat{f}$ denote the Fourier transform of f, and let $\mathcal{F}^{-1}(\hat{f})$ denote the inverse transform, viz.

$$\hat{f}(\xi) = (\mathcal{F})(\xi) = \int_{-\infty}^{\infty} f(x) e^{-2\pi i x \xi} dx$$

$$f(x) = (\mathcal{F}^{-1}\hat{f})(x) = \int_{-\infty}^{\infty} \hat{f}(\xi) e^{2\pi i x \xi} d\xi$$

and analogously in three dimensions. In this text, the symbol ξ is used exclusively to denote an argument of a Fourier transformed function, i.e. a *Fourier space coordinate*.

The utility of the Fourier transform when analyzing differential equations is that differential operators in ordinary space turn into multiplication operators in Fourier space. This reduces partial differential equations (PDEs) in space and time to ordinary differential equations (ODEs) in time for which straightforward numerical methods often can be used. With slight abuse of notation,

$$\mathcal{F}\left[\frac{\partial}{\partial x}\right] = i\xi$$

$$\mathcal{F}\left[\frac{\partial^2}{\partial x^2}\right] = -|\xi|^2$$

and in n dimensions, the gradient and Laplace operators become

$$\mathcal{F}\left[\nabla\right] = i\xi = i(\xi_1, \ldots, \xi_n)$$

$$\mathcal{F}\left[\Delta\right] = -|\xi|^2 = -\left(|\xi_1|^2 + \ldots + |\xi_n|^2\right).$$

From the physical point of view, the Fourier transform translates from ordinary space, described by the coordinates $\mathbf{x} = (x, y, z)$, to momentum space or Fourier space. In the latter space, the momentum operator $\mathbf{p} = -i\hbar\nabla$ reduces to multiplication by the momentum coordinate vector $\mathbf{p} = \xi = \hbar(\xi_1, \xi_2, \xi_3)$, and in particular, $\mathbf{p} = \xi$ if we choose $\hbar = 1$. In analogous fashion, the Fourier transform with respect to time translates between time and energy.

A.2 Diagonalization

Matrix operators, such as the Dirac operator, are often most effectively analyzed via diagonalization. Differential matrix operators, such as the free Dirac operator, can be diagonalized in similar to fashion to ordinary matrices by transforming them to Fourier space.

A square matrix A is diagonalizable if there exists a matrix P and diagonal matrix D such that $A = PDP^{-1}$. Diagonalizing A amounts to finding a basis of eigenvectors of A: more precisely, P is the concatenation of the eigenvectors of A, and the diagonal of D contains the corresponding eigenvalues. Since $(aP)^{-1} = a^{-1}P$, the matrices P and P^{-1} can both be chosen so as to be unitary, which is sometimes convenient.

Diagonalization is useful for computation of matrix or operator exponentials, and often gives more information than direct application of the exponential power series. It is easy to show that $A^k = PD^kP^{-1}$, and therefore

$$e^A = \sum_{k=0}^{\infty} \frac{A^k}{k!} = \sum_{k=0}^{\infty} \frac{1}{k!} PD^kP^{-1} = P\left(\sum_{k=0}^{\infty} \frac{1}{k!} D^k\right) P^{-1} = Pe^DP^{-1}.$$

The exponential of a diagonal matrix is the elementwise exponential, and therefore also e^A can be computed. Likewise, qualitative information about e^A is obtained from the eigenvalues. Diagonalization works for other analytic functions of matrices besides the exponential function.

B Wavefunction snapshots

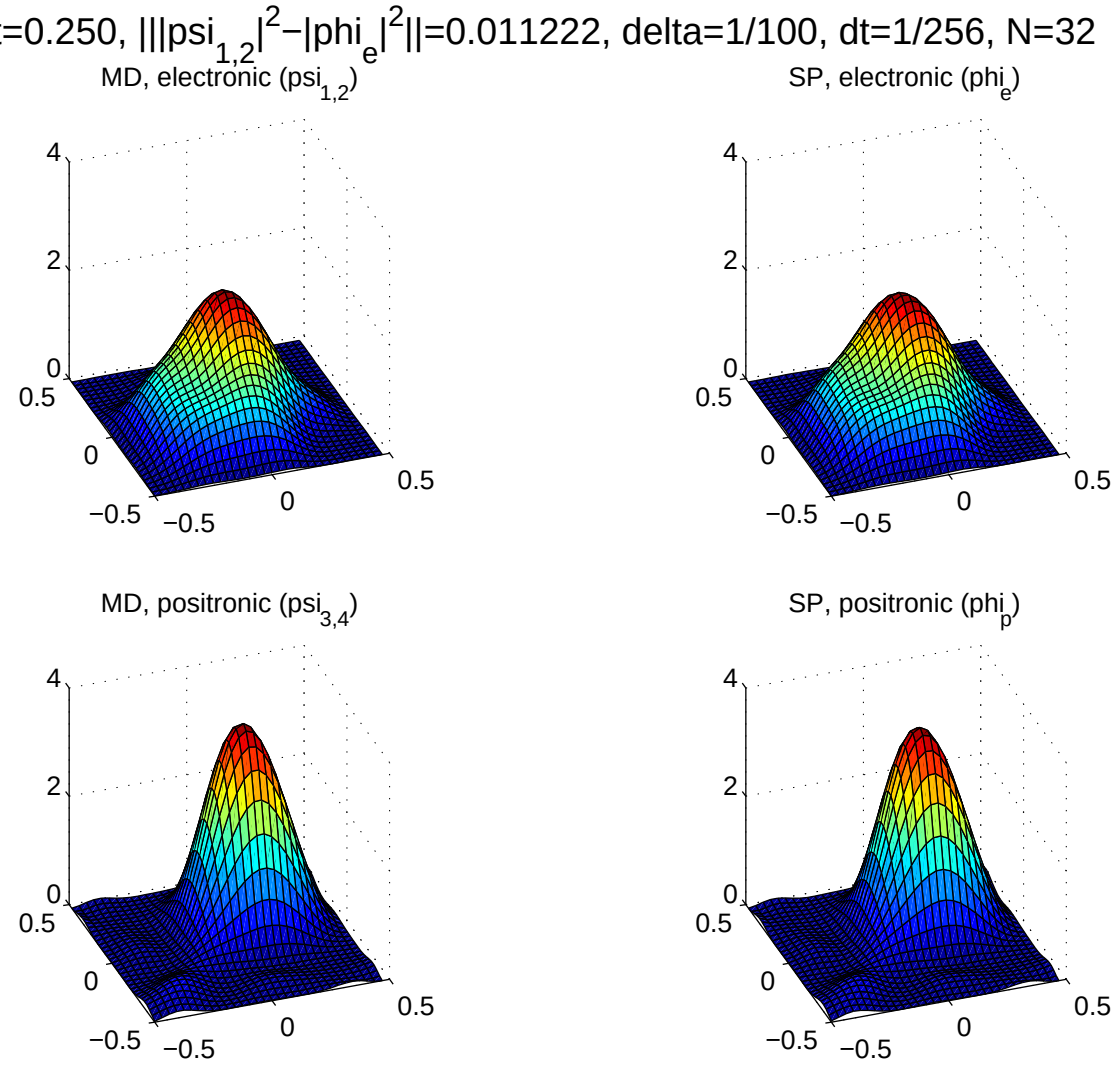

Figure 4: Snapshot of time evolution of the Maxwell-Dirac and Schrödinger-Poisson systems, with nonrelativistic parameter $\delta = 1/100$ for MD. The left hand side shows $\|\psi_1\|^2 + \|\psi_2\|^2$ and $\|\psi_3\|^2 + \|\psi_4\|^2$ with the probability amplitude in the z-direction integrated onto the x, y-plane. The right hand side shows $\|\phi_e\|^2$ and $\|\phi_p\|^2$.

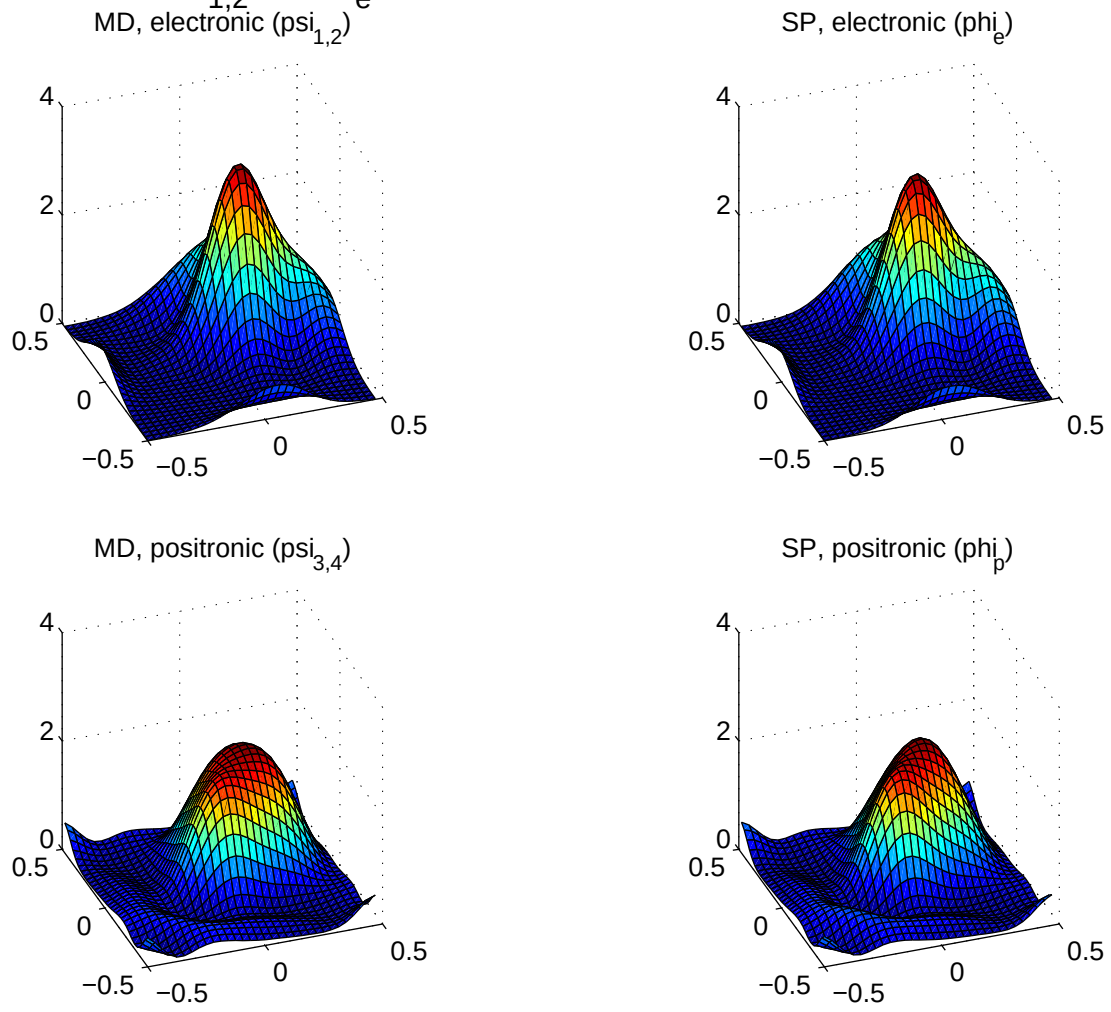

Figure 5: Snapshot of MD and SP, time $t = 0.75$. See caption of figure 4 for additional information.

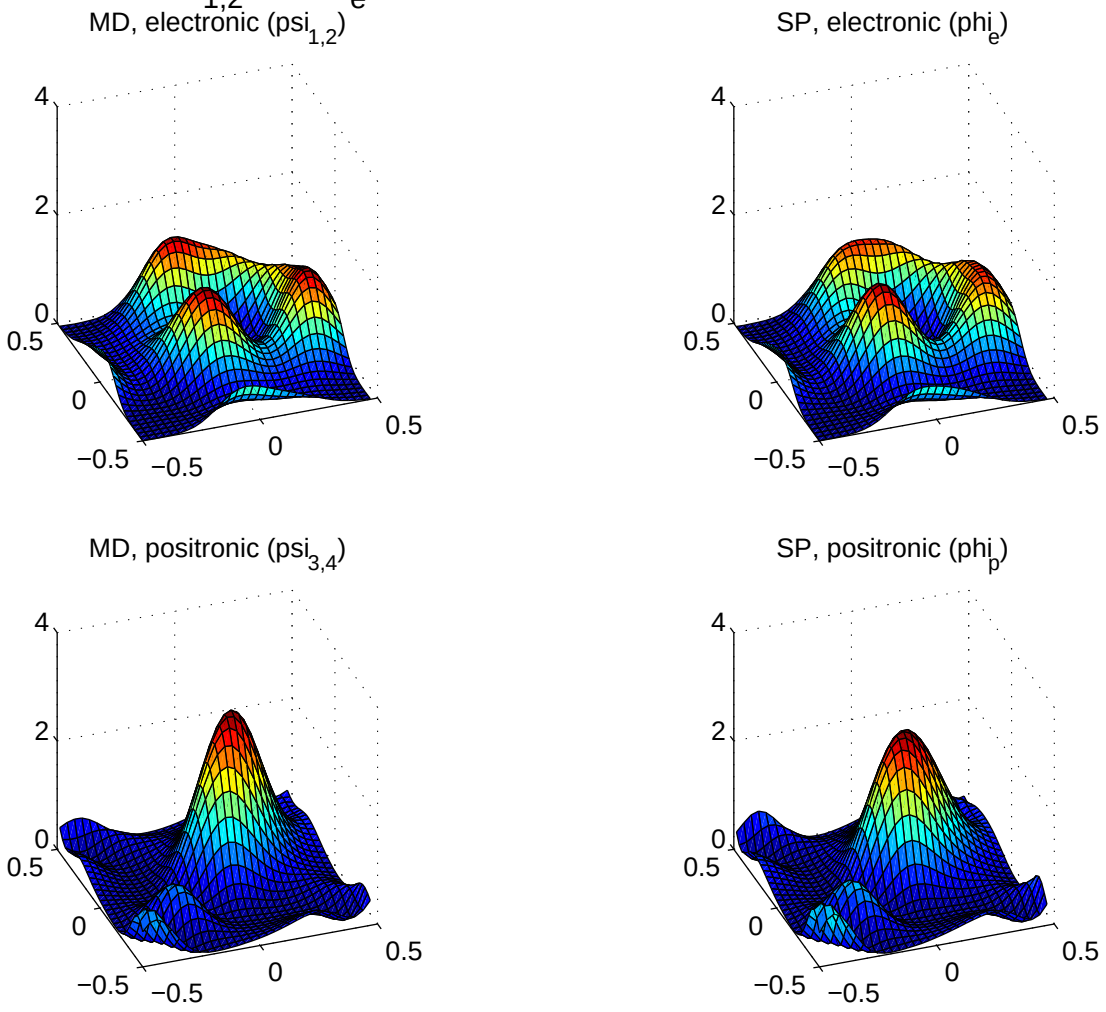

Figure 6: Snapshot of MD and SP, time $t = 1.0$. See caption of figure 4 for additional information.

C Source code

C.1 Example usage

```
% demo.m

epsilon = 1.0;
delta = 0.01;
dt = 1./128;
N = 32;
[space, fspace] = md_domain([-0.5,0.5],[-0.5,0.5],[-0.5,0.5],N);
x = space{1};
y = space{2};
z = space{3};
zero = x.*0;
xyz2 = x.^2 + y.^2 + z.^2;
volume = 1;

% Initial wavefunction
wv_e = cos(pi*(x+0.1)).^4 .* cos(pi*(y+0.1)) .^ 4;
wv_p = cos(pi*(x-0.1)).^4 .* cos(pi*(y-0.1)) .^ 4;

psi{1} = wv_e;
psi{2} = zero;
psi{3} = wv_p;
psi{4} = zero;

phi_e = wv_e;
phi_p = wv_p;

% Initial potentials
V = zero;
dV = zero;
for i=1:3
    A{i} = zero;
    dA{i} = zero;
end

TMAX = 1;
clear M;
n = 0;
t = 0.0;

t_hist = [];
e_err_hist = [];
p_err_hist = [];
mde_hist = {};
mdp_hist = {};
spe_hist = {};
spp_hist = {};

while t < TMAX
```

```
    n = n + 1;
    t = t + dt;
    Vex = 5 * sin(pi*x).^4 .* sin(pi*y).^4;
    Aex = {0, 0, 0};
    [psi, V, dV, A, dA] = md_step(psi, V, dV, A, dA, ...
        space, fspace, dt, epsilon, delta, Vex, Aex);
    [phi_e, phi_p] = sp_step(phi_e, phi_p, Vex, dt, ...
        space, fspace);
    abspsi = md_abs2(psi);
    psinorm = sum(abspsi(:)) * volume / N^3;
    clf;
    hold on;
    wvplot(x, y, N, {psi{1},psi{2}}, psinorm, 2, 2, 1, ...
        'MD, electronic (psi_{1,2})');
    wvplot(x, y, N, {psi{3},psi{4}}, psinorm, 2, 2, 3, ...
        'MD, positronic (psi_{3,4})');
    wvplot(x, y, N, {phi_e}, psinorm, 2, 2, 2, ...
        'SP, electronic (phi_e)');
    wvplot(x, y, N, {phi_p}, psinorm, 2, 2, 4, ...
        'SP, positronic (phi_p)');
    drawnow;
end
```

C.2 MD and SP solvers

```
% md_step.m

% Given solution of MD system at time t,
% compute solution at time t + dt.
% Vex and Aex are given external potentials at time t + dt.
%
% V and dV are single arrays
% A and dA are 3-item cell arrays for A1, A2, A3
% psi is a 4-item cell array for psi1, psi2, psi3, psi4
%
% space and fspace are coordinates, as computed by md_domain
% epsilon and delta are scale parameters for asymptotic solution

function [psi_new, V_new, dV_new, A_new, dA_new] = ...
    md_step(psi_n, V_n, dV_n, A_n, dA_n, ...
    space, fspace, dt, epsilon, delta, Vex, Aex)

% Fourier transform of psi
for i=1:4
    psihat_n{i} = fftn(psi_n{i});
end

% Forward exponential matrix
M = md_expmatrix1(epsilon, delta, fspace, dt);
for i=1:4
    phihat_new{i} = M{i,1}.*psihat_n{1} + M{i,2}.*psihat_n{2} + ...
                    M{i,3}.*psihat_n{3} + M{i,4}.*psihat_n{4};
end
```

```
% Inverse Fourier transform of phi_{n+1}
for i=1:4
    phi_new{i} = ifftn(phihat_new{i});
end

% Compute current and particle densities
% 2.21
% rho_n = |psi_n|^2
% rho_{n+1} = |phi_{n+1}|^2
rho_n = md_abs2(psi_n);
rho_new = md_abs2(phi_new);
J_n = md_diracprod(delta, psi_n);
J_new = md_diracprod(delta, phi_new);

% FFT
Vhat_n = fftn(V_n);
dVhat_n = fftn(dV_n);
rhohat_n = fftn(rho_n);
rhohat_new = fftn(rho_new);
for i=1:3
    Ahat_n{i} = fftn(A_n{i});
    dAhat_n{i} = fftn(dA_n{i});
    %Jhat_n{i} = fftn(J_n{i});
    %Jhat_new{i} = fftn(J_new{i});
    Jhat_sum{i} = fftn(J_n{i} + J_new{i});
end

% Update A and V with the Crank-Nicolson method
% 2.19-2.21

% Crank-Nicolson update matrix, (2.19)
% This could be precomputed for fixed dt, but it's a small
% part of the total computation time anyway.
% |xi|^2
absxi2 = md_abs2(fspace);
CN_factor = 1 ./ (1 + (dt^2 * absxi2 / (4*delta^2)));
CN_M11 = 1 - (dt^2 * absxi2 / (4*delta^2));
CN_M12 = dt;
CN_M21 = -dt*absxi2/delta^2;
CN_M22 = 1 - (dt^2 * absxi2 / (4*delta^2));
CN_B1 = epsilon * dt^2 / (4*delta^2);
CN_B2 = epsilon * dt / (2*delta^2);
% End CN update matrix

BV = rhohat_n + rhohat_new;
Vhat_new  = (CN_M11.*Vhat_n+CN_M12.*dVhat_n+CN_B1.*BV).*CN_factor;
dVhat_new = (CN_M21.*Vhat_n+CN_M22.*dVhat_n+CN_B2.*BV).*CN_factor;
for i=1:3
    %BA = delta *  (Jhat_n{i} + Jhat_new{i});
    BA = delta * Jhat_sum{i};
    Ahat_new{i}  = (CN_M11.*Ahat_n{i} + CN_M12.*dAhat_n{i} + ...
        CN_B1.*BA) .* CN_factor;
```

```
    dAhat_new{i} = (CN_M21.*Ahat_n{i} + CN_M22.*dAhat_n{i} + ...
        CN_B2.*BA) .* CN_factor;
end

% Updated V and A and their derivatives
V_new = ifftn(Vhat_new);
dV_new = ifftn(dVhat_new);
for i=1:3
    A_new{i} = ifftn(Ahat_new{i});
    dA_new{i} = ifftn(dAhat_new{i});
end

M = md_expmatrix2(epsilon, delta, V_new, Vex, A_new, Aex, dt);
for i=1:4
    psi_new{i} = M{i,1}.*phi_new{1} + M{i,2}.*phi_new{2} + ...
                 M{i,3}.*phi_new{3} + M{i,4}.*phi_new{4};
end

% Possibly remove imaginary noise
V_new = real(V_n);
dV_new = real(dV_n);
for i=1:3
    A_new{i} = real(A_new{i});
    dA_new{i} = real(dA_new{i});
end

% sp_step.m

function [phi_e,phi_p] = sp_step(phi_e, phi_p, Vex, ...
    dt, space, fspace)

x=space{1};
y=space{2};
z=space{3};
px=fspace{1};
py=fspace{2};
pz=fspace{3};

xi2 = px.^2 + py.^2 + pz.^2;

% Solve i * (d/dt) phi_{e/p} = (-/+ Delta/2) phi_{e/p}
phi_e = ifftn( exp(-0.5i*xi2*dt) .* fftn(phi_e) );
phi_p = ifftn( exp(0.5i*xi2*dt) .* fftn(phi_p) );

% Poisson's equation
% -Delta V = |phi_p|^2 + |phi_e|^2
Vhat = fftn( abs(phi_e).^2 + abs(phi_p).^2 ) ./ xi2;
Vhat(1,1,1) = 0;
V = ifftn(Vhat);

% Solve i * (d/dt) phi_{e/p} = (V + Vex) phi_{e/p}
phi_e = exp(-1i*dt*(V+Vex)) .* phi_e;
phi_p = exp(-1i*dt*(V+Vex)) .* phi_p;
```

```
% md_expmatrix1.m
% Note: formulas refer to the paper by Huang et al.

function M = md_expmatrix1(epsilon, delta, xi, dt)
xi1 = xi{1};
xi2 = xi{2};
xi3 = xi{3};
% |xi|^2
absxi2 = xi1.*xi1 + xi2.*xi2 + xi3.*xi3;
% |epsilon * delta * xi|^2
absepsdeltaxi2 = absxi2 * epsilon^2 * delta^2;
% 2.16
lambda = 1i/(epsilon*delta^2)*sqrt(1+epsilon^2*delta^2*absxi2);
% 2.18
cl = cos(-1i*lambda*dt);
sl = sin(-1i*lambda*dt) .* ((1+absepsdeltaxi2) .^ (-0.5));
M = cell(4,4);
% 2.17
M{1,1} = cl - 1i.*sl;
M{1,2} = 0;
M{1,3} = -1i .* epsilon .* delta .* sl .* xi3;
M{1,4} = -epsilon .* delta .* sl .* (xi2+1i.*xi1);
M{2,1} = 0;
M{2,2} = cl - 1i*sl;
M{2,3} = epsilon .* delta .* sl .* (xi2-1i.*xi1);
M{2,4} = 1i .* epsilon .* delta .* sl .* xi3;
M{3,1} = -1i .* epsilon .* delta .* sl .* xi3;
% note: typo in paper
M{3,2} = -epsilon .* delta .* sl .* (xi2+1i.*xi1);
M{3,3} = cl + 1i.*sl;
M{3,4} = 0;
M{4,1} = epsilon .* delta .* sl .* (xi2-1i.*xi1);
M{4,2} = 1i .* epsilon .* delta .* sl .* xi3;
M{4,3} = 0;
M{4,4} = cl + 1i.*sl;

% md_expmatrix2.m

% Compute the second exponential matrix
function M = md_expmatrix2(epsilon, delta, V, Vex, A, Aex, dt)
V = V + Vex;
A1 = A{1} + Aex{1};
A2 = A{2} + Aex{2};
A3 = A{3} + Aex{3};
M = cell(4,4);
Aabs = sqrt(abs(A1).^2 + abs(A2).^2 + abs(A3).^2);
%RA = 1 ./ Aabs;
RA = A1 * 0;
% Note: this is a normalization constant. Where 1/|A| is undefined,
% the corresponding component in the matrix will be zero.
for k=1:numel(Aabs)
    if Aabs(k) == 0
        RA(k) = 0;
```

```
    else
        RA(k) = 1./Aabs(k);
    end
end
B1 = A1 .* RA;
B2 = A2 .* RA;
B3 = A3 .* RA;
u = Aabs .* dt ./ epsilon;
v = dt .* V ./ epsilon;
su = sin(u);
cu = cos(u);
sv = sin(v);
cv = cos(v);
a = cv-1i.*sv;
b = 1i.*cv + sv;
M{1,1}=cu.*a; M{1,2}=0;
M{1,3}=B3.*su.*b; M{1,4}=(1i.*B1+B2).*su.*a;
M{2,1}=0; M{2,2}=M{1,1};
M{2,3}=(B1+1i.*B2).*su.*b; M{2,4}=-1i.*B3.*su.*a;
M{3,1}=M{1,3}; M{3,2}=M{1,4}; M{3,3}=M{1,1}; M{3,4}=0;
M{4,1}=M{2,3}; M{4,2}=M{2,4}; M{4,3}=0; M{4,4}=M{1,1};

% md_domain.m

% space--3-item cell array of space cooordinates [x,y,z]
% fspace--3-item cell array of Fourier coordinates [xi1,xi2,xi3]
% each coordinate array is N x N x N
function [space, fspace] = md_domain(xd, yd, zd, N)

pos_x1 = xd(1); pos_x2 = xd(2);
pos_y1 = yd(1); pos_y2 = yd(2);
pos_z1 = zd(1); pos_z2 = zd(2);
xwidth = pos_x2 - pos_x1;
ywidth = pos_y2 - pos_y1;
zwidth = pos_z2 - pos_z1;
%volume = xwidth * ywidth * zwidth;

xs = linspace(pos_x1, pos_x2, N+1); xs = xs(1:N);
ys = linspace(pos_y1, pos_y2, N+1); ys = ys(1:N);
zs = linspace(pos_z1, pos_z2, N+1); zs = zs(1:N);
[xx, yy, zz] = ndgrid(xs, ys, zs);

% Coordinates xi in Fourier (momentum) space
% Note that the Fourier modes range from -N/2+1 to N/2, but
% the FFT indexing starts at 0, so there is wraparound.
pv = [];
for p=0:N-1
    if p < floor(N/2)
        pv(p+1) = p;
    else
        pv(p+1) = p - N;
    end
end
```

```
[xi1,xi2,xi3] = ndgrid(2*pi*pv/xwidth,2*pi*pv/ywidth,...
    2*pi*pv/zwidth);

space = cell(3,1);
fspace = cell(3,1);

space{1} = xx;
space{2} = yy;
space{3} = zz;

fspace{1} = xi1;
fspace{2} = xi2;
fspace{3} = xi3;
```

C.3 Helper files

```
% md_abs2.m

function y = md_abs2(x)
    y = 0;
    for i=1:length(x)
        y = y + abs(x{i}).^2;
    end
end

% md_diracprod.m

% Computes {Y_1, Y_2, Y_3} where Y_k = <X, alpha^k X> / c
% where <x,y> is the C^4 inner product with x conjugated
% alpha^k is a Dirac matrix
function Y = md_diracprod(c, X)
    Y = cell(3,1);
    A1 = conj(X{1});
    A2 = conj(X{2});
    A3 = conj(X{3});
    A4 = conj(X{4});
    Y{1} = A1.*X{4} + A2.*X{3} + A3.*X{2} + A4.*X{1};
    Y{2} = i*(A2.*X{3} + A4.*X{1} - A1.*X{4} - A3.*X{2});
    Y{3} = A1.*X{3} + A3.*X{1} - A2.*X{4} - A4.*X{2};
    Y{1} = Y{1} / c;
    Y{2} = Y{2} / c;
    Y{3} = Y{3} / c;
end

% flatten2.m

function y = flatten2(f, N)

abspsi = md_abs2(f);
y = abspsi(:,:,1);
for i=2:N
    y = y + abspsi(:,:,i);
```

```
end
y = y / N;

% wvplot.m

function data = wvplot(x, y, N, f, fnorm, srows, scols, sn, msg)

subplot(srows,scols,sn);
Z = flatten2(f, N) ./ fnorm;
surf(x(:,:,N/2), y(:,:,N/2), Z);
zlim([0,4]);
view(-20,30);
pbaspect([1 1 1]);
title(msg);
data = Z;
```

References

[1] Weizhu Bao and Xiang-Gui Li. An efficient and stable numerical method for the Maxwell-Dirac system. *J. Comput. Phys.*, 199(2):663–687, 2004.

[2] Philippe Bechouche, Norbert J. Mauser, and Sigmund Selberg. On the asymptotic analysis of the Dirac-Maxwell system in the nonrelativistic limit. *J. Hyperbolic Differ. Equ.*, 2(1):129–182, 2005.

[3] Zhongyi Huang, Shi Jin, Peter A. Markowich, Christof Sparber, and Chunxiong Zheng. A time-splitting spectral scheme for the Maxwell-Dirac system. *J. Comput. Phys.*, 208(2):761–789, 2005.

[4] Nobert J. Mauser and Sigmund Selberg. Convergence of the Dirac-Maxwell system to the Vlasov-Poisson system. *Communications in PDE*, 32(3):503–524, 2007.

[5] Karl Michael Schmidt. Eigenvalues in gaps of perturbed periodic Dirac operators: numerical evidence. *J. Comput. Appl. Math.*, 148:169–181, November 2002.

[6] C. Sparber and P. Markowich. Semiclassical asymptotics for the Maxwell-Dirac system, 2003. arXiv:math-ph/0305009v1.

[7] M. H. Stone. On one-parameter unitary groups in Hilbert space. *Ann. of Math. (2)*, 33(3):643–648, 1932.

[8] Paul Strange. *Relativistic quantum mechanics*. Cambridge University Press, Cambridge, 1998.

[9] Bernd Thaller. *The Dirac Equation*. Texts and Monographs in Physics. Springer-Verlag, Berlin, 1992.